

initial set-up of the system which required half of the first night. As for the previous scientific observing run (November 1990) the system worked for the astronomers in a fully reliable and reproducible way. During these observations the seeing conditions varied from good to excellent. Unfortunately, during part of the observing time the programme suffered under cloud coverage.

The scientific goals of the November 1990 run concentrated on the solar system (i.e. Pallas), extragalactic astronomy (i.e. NGC 1068), and the search for brown and red dwarfs (i.e. G29-38, G1866). For this run the major interests were in the area of circumstellar features (i.e. Z CMa, FU Ori, VY CMa), jets (Red Rectangle), and ejected material from

luminous blue variables (i.e. η Car, AG Car). Out of this list of objects one of the most exciting was η Carinae, where new amazing structures of arcsecond scale have been revealed around the central object in the L- (3.8 μm) and M-band (4.5 μm) (see Figure).

In addition, during the test and set-up, night images were taken in the visible wavelength band with a commercial CCD. These experiments demonstrated that even in this range a significant improvement in image quality (corrected image FWHM ~ 0.4 arcsec for an initial seeing of ~ 0.7 arcsec) was possible with the current prototype system.

The last and final run with the current prototype system is planned for April this year. Extensive technical tests will be performed before the system goes

back to Europe for a major upgrade programme (Called COME-ON PLUS). It will be equipped with a fifty actuator mirror and a modified wavefront computer to reach 40 Hz closed-loop bandwidth. This will allow to produce diffraction-limited images at shorter wavelengths, typically down to 1.7 μm . All optical parts will receive new, more efficient coatings, pushing the limiting magnitude for the reference star up to magnitude 14. This upgrade will make the VLT adaptive optics prototype system a very powerful tool for higher angular resolution observation of the southern sky.

G. GEHRING, ESO
F. RIGAUT, Observatoire de Paris-Meudon

New 2D Array Detectors Installed in IRSPEC and IRAC

A. MOORWOOD, ESO, Garching

A. MONETI and R. GREDEL, ESO, La Silla

IRSPEC at the NTT and IRAC at the 2.2-m telescope were equipped with new SBRC 58 \times 62 InSb and Philips Components 64 \times 64 Hg:Cd:Te arrays respectively during late January and early February. In the case of IRSPEC the new array has not only brought more than an order of magnitude s/n gain at $\lambda < 2.5 \mu\text{m}$ but also provides a long-slit capability which both extends the scientific capabilities of the instrument and simplifies its operation compared with the old 1D array which it has replaced. The present upgrading of these instruments has, at some risk, been done between normally scheduled observing runs in order to keep them available for visitors and so that they can benefit from any improved performance as soon as possible. Due to the need to complete this article within a few days of the end of both test runs we are only able at this stage to present a few preliminary results based on partially reduced data at the telescope but will report more fully in a future issue of the *Messenger*. In the present evolutionary stage of infrared arrays, however, the situation can change rather rapidly. New InSb arrays have already been received and will be tested as soon as possible in Garching and a 256 \times 256 Hg:Cd:Te array should be delivered later this year. Visitors planning to apply for observing time are therefore encouraged to contact Alan Moorwood in Garching or the astronomers responsible on La Silla – Roland

Gredel and Andrea Moneti for IRSPEC and IRAC respectively for the latest information. (EMail: @DGAESO51 or ESOM-C1::ALAN or RGREDEL or MONETI).

IRSPEC

New Features at the NTT

In its new home at the NTT IRSPEC is attached permanently to the telescope structure (and hence free of instrumental flexure effects) and employs an optical de-rotator in front of the slit to counter the field rotation at the telescope Nasmyth focus and to permit orientation of the slit at any position angle on the sky. The detector pixels of 76 μm are a factor of 2.7 smaller than in the old array, corresponding to $\sim 2''.2$ on the sky, and the maximum slit length using all 58 pixels in the cross dispersion direction would therefore correspond to $\sim 2'$. Unfortunately only the central $1'$ at present is free of vignetting – believed to be mainly due to a radiation stop installed several years ago when the slit was only 6" long! This will be removed as soon as possible. Alignment of the slit and de-rotator to the telescope optical axis (rotation axis) was achieved within $1''$ and combined telescope/de-rotator tracking errors in the worst case of objects transiting within 1° of zenith were measured to be less than $1''$. For objects with accurately known coordinates the excellent NTT pointing does

pose a small problem in that they usually disappear in the slit which then has to be closed in order to see them!

For calibration purposes the slit can be illuminated by an integrating sphere equipped with spectral line lamps plus a halogen lamp and black body source for flat fielding which is mounted in the telescope adapter and viewed via a retractable diverter mirror.

During the recent test the IRSPEC functions were controlled via an HP1000 computer using the existing software while the detector integration parameters were set by form filling on the A900 instrument computer with status display on a RAMTEK monitor which is also used to control the measurements (start, stop, repeat, etc.) by 'mouse' clicking on a menu bar. In future all parameters will be set via the A900. IHAP is available on-line with a RAMTEK monitor for image display and a graphics terminal for obtaining 1D spectrum plots, traces, etc. In addition, images and 1D traces can be displayed in real time on a monitor connected directly to the pre-processor in the detector acquisition system. Cut levels and any averaging desired for the 1D display, e.g the spectrum averaged over n pixels along the slit can be easily set via the A900 terminal and the monitor automatically displays the coordinates and value of the pixel (plus values of the surrounding pixels) indicated by a mouse driven arrow.

From the observers point of view the new system now resembles much more closely an optical spectrograph. Neither sky chopping nor a chart recorder were used during the test (although the possibility of retaining sky chopping to improve the cancellation of sky lines is being considered). Visible objects were normally centred (or generally found to be centred) using the slit viewing camera while invisible ones were centred either by blind pointing or offsetting from a nearby star. If necessary, the real time monitor can be used in place of the chart recorder for infrared 'peaking-up'. In order to perform sky subtraction, sufficiently compact objects were observed alternately at two positions along the slit thus yielding positive and negative images after subtraction and hence no loss of on-object integration time. For very extended regions it was necessary to choose appropriate sky positions at larger distances.

Performance

The SBRC 58×62 pixel InSb array now installed has a quantum efficiency ~ 0.8 around $2 \mu\text{m}$, exhibits its nominal read noise of $\sim 500\text{e}$ and dark current of $\sim 200\text{e/s}$ at 30 K and has 17 bad pixels. As the pixel pitch of $76 \mu\text{m}$ is a factor of 2.7 smaller than in the old 1D array, the resolving power is effectively higher by the same ratio, i.e. $\sim 2500\text{--}5000$ depending on wavelength and grating order. However, this definition corresponds to a slit width equal to one pixel whereas most of the test observations were made with two pixel matching to a slit of 4.5 yielding resolving powers of half these values i.e. close to the values defined with the old detector but now with adequate sampling, at least for extended sources.

Figure 1 shows a sky subtracted 'image' obtained with the slit oriented across the Orion bar as an example of what can be displayed on-line at the telescope on the real time monitor and/or the RAMTEK display. The slit is in the Y direction and dispersion in the X direction. In the upper part of the image the diffuse band is continuum emission from ionized gas behind the ionization front which also shows He I and some 1-OS(1) H_2 line emission which then increases in intensity into the molecular cloud ahead of the front. A more compact continuum source which also exhibits He I emission can be seen in the lower part and could be a compact H II region in or in front of the molecular cloud. Total on-source integration time was $5 \times 60\text{s}$ and the peak intensities/pixel on the He I and H_2 lines in the upper ionized region are comparable and $\sim 5 \cdot 10^{-22} \text{ W.cm}^{-2}$.

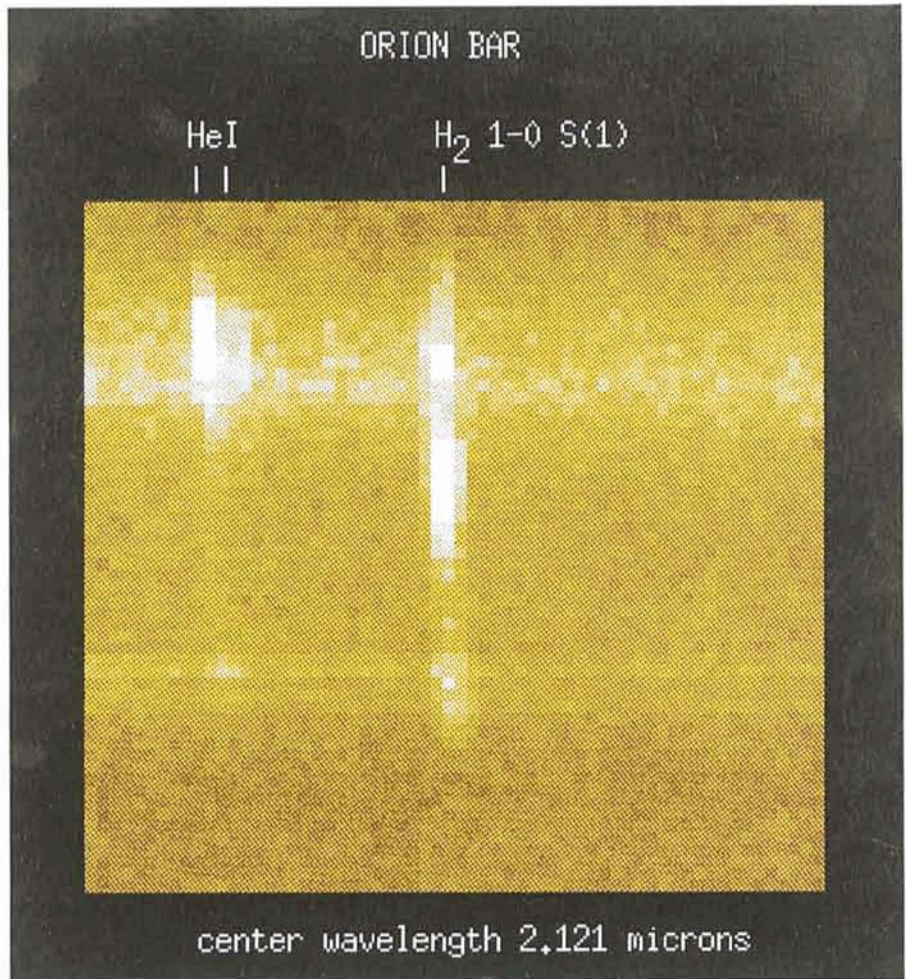


Figure 1: Sky subtracted IRSPEC 'image' with the slit oriented across the Orion bar. Towards the top can be seen both extended continuum and He I line emission from ionized gas behind the ionization front plus H_2 1-OS(1) line emission which then extends downwards into the molecular cloud and increases in strength. Another continuum source exhibiting He I emission, which could be an ultracompact H II region within or in front of the molecular cloud, is also visible towards the bottom. Total on-source integration time was $5 \times 60\text{s}$ and the peak intensities/pixel on the He I and H_2 lines in the upper ionized region are comparable and $\sim 5 \cdot 10^{-22} \text{ W.cm}^{-2}$.

Except for standard stars the typical on-chip integration times used for measurements at $\lambda < 2.5 \mu\text{m}$ were typically 60s and after subtraction of a sky frame corresponding to the same integration time the 1σ noise corresponded to $J \sim 13.25 \text{ mag.} = 3 \cdot 10^{-22} \text{ W.cm}^{-2}/\text{pixel}$, $H \sim 14.25 \text{ mag.} = 8 \cdot 10^{-23} \text{ W.cm}^{-2}/\text{pixel}$, $K \sim 13.75 \text{ mag.} = 7 \cdot 10^{-23} \text{ W.cm}^{-2}/\text{pixel}$ and $L \sim 8 \text{ mag.} = 3 \cdot 10^{-21} \text{ W.cm}^{-2}/\text{pixel}$. Except at L, where photon noise on the sky emission dominates, these limits are about a factor of 15 fainter than quoted in the old IRSPEC manual for the same integration time! If the sky frame also contains the object at a different position along the slit it is possible to gain a further factor of 1.4 whereas integrating over the same aperture as subtended by the old pixels will, in principle, lead to a factor of 2-3 increase in the effective noise. Although this already represents a large sensitivity gain relative to the old detector it is still hoped to improve on this substantially in the future. At pres-

ent the noise for 60s integrations is a combination of the nominal detector read noise and shot noise on the thermal background in the instrument which was found to be much higher than expected - partly due to the instrument itself running warmer than usual (following an obviously unsuccessful attempt to simplify the cryogenic system!) and partly due to insufficient shielding close to the detector. As a next step therefore it is planned to (i) implement multiple non-destructive sampling of the detector which can substantially reduce the read noise and has been tried briefly in the laboratory but was not ready for implementation during this first telescope test and (ii) introduce a number of measures to reduce the internal thermal background.

In addition to the s/n considerations discussed above it should be borne in mind that other factors such as flat fielding and cancellation of sky emission lines can, depending in detail on the

nature of the observation, also effect the overall system performance. During this first test, the halogen lamp at $\lambda < 2.5 \mu\text{m}$ and the sky at longer wavelengths were used for flat fielding. A few checks made on line indicate that these techniques provide correction to better than 1% but more analysis of the data is required in order to establish the actual limits and optimum procedures. No attempt has been made so far either to connect frames at different grating settings to produce continuous spectra. (In this latter regard, the old 'vignetting' problem should be considerably reduced because of the possibility of integrating over several pixels along the slit if necessary.) Residual sky lines (mainly OH at $\lambda < 2.5 \mu\text{m}$ and H₂O at longer wavelengths) were still found to be present in some regions on object/sky difference frames separated in time by 5-10 min. Depending on the programme this may or may not be a problem but if it is, the sky reference can be measured more often or it should be possible to further suppress the residuals using 'sky' measurements within the flat fielded frames themselves. In this regard, however, it should be noted that due to the Littrow mount used in IRSPEC, spectral lines are observed to be parallel to the array at wavelengths corresponding to the grating blaze angle but can be tilted by up to 8 degrees at the extreme ends of the grating range.

In summary, IRSPEC now has both considerably improved sensitivity, which it is hoped to increase further in future, and extended scientific capabilities (due to the long slit). It is also simpler to operate but whether this is also true of the data reduction remains to be seen.

IRAC

As the new Philips Components 64×64 Hg:Cd:Te array only arrived about 10 days before the planned test there was relatively little time available to characterize and optimize it before it was installed on the 2.2-m telescope. Nevertheless, some laboratory measurements were made and yielded a read noise ~ 400 e, a dark current of ~ 1000 e/s (at 50K), about 20-100 bad pixels depending on integration time in the range 1 to 60s and an efficiency (q.e \times fill factor) of $\sim 20\%$. Although fewer bad pixels would have been nice, the only real disappointment in these numbers was the efficiency which was expected to be closer to 50%. Overall, however, the larger format together with the fact that this array operates out to $4.2 \mu\text{m}$ (with a large well capacity $\sim 10^7$ e) and appears to be rather uniform and stable represents a consid-

erable improvement compared with the 32×32 array which it replaces.

At the telescope the 'warm' (i.e. high dark current) pixels are obvious in the raw images and also exhibit 'tails' presumably indicative of some charge transfer problem in the CCD readout chip to which the Hg:Cd:Te array is bonded. Sky subtraction leads to good cancellation of the tails and the warm pixels themselves can be removed with a high cut median filter either on-line or later. (By adjusting the drive voltages it is also possible to substantially reduce the number of warm pixels at the expense of creating a roughly equal number of 'cold' ones which are preferable because they are less visually obvious and do not create tails). Where the tails do potentially cause some problems is for observations of bright stars which also show this effect at least in the J and H bands.

It is not possible here to give reliable limiting magnitudes for the various modes (IRAC is equipped with broadband filters and CVF's which can be combined with on-line selectable magnifications of 0'3, 0'5, 0'8 and 1'6/pixel). As a guide however, based on measurements with a detector integration time of 60s and with 0'8 pixels, it appears possible to do photometry at $s/n=5$ in a 50 pixel synthetic beam down to $K=15$ and $J \sim H \sim 15.5-16$ on frames obtained with a total integration time of 1 hr equally divided between object and sky. For broadband L ($3.8 \mu\text{m}$) imaging the corresponding value is $L=9$ mag using 1 sec integrations and 0'5 pixels. Based on the actual detector parameters and overall efficiency measured on stars, the overall performance should actually be better, and this discrepancy is still not fully understood. It appears however that the actual read noise at the telescope was probably 2-3 times higher than measured in the laboratory and that this may have followed changes to settings to the acquisition system. The sky/telescope background also appeared to be high and, at least at K and L, could be attributable to the extremely high telescope temperature ($\sim 16\text{C}$) during the test run. It is therefore likely that the above figures are, if anything, on the pessimistic side. In addition to broad-band imaging, some tests were also made with the CVF and the K band Fabry Perot. As several people have expressed interest in $3.28 \mu\text{m}$ feature observations, the CVF performance at this wavelength was tested specifically by observing the planetary nebula IC 418 which, unfortunately, could not be detected in 15 min. This is presumably due to the relatively low transmission of our CVF in this region and means that, for the time being, we would not

encourage people to propose specifically for such observations.

In summary, IRAC is now both much better and much easier to work with than before and its performance can probably be improved beyond the preliminary guide given here once we have more experience in how to best optimize this particular array. It is also not excluded that this array could be replaced in the future with one of the InSb arrays still to be tested in Garching if this would lead to a substantial improvement in the overall performance. As this would require technical effort, however, this decision also depends on the future progress of IRAC2 and the actual delivery of its 256×256 Hg:Cd:Te array which is now ordered and expected before the end of the year.

Acknowledgements

At the risk of omitting to mention several people who contributed to the work described here we would like to specially thank P. Biereichel, M. Comin, G. Finger, H. Gemperlein, J.-L. Lizon, M. Meyer and U. Weilenmann for their technical support during these two parallel test runs and also our night assistants J. Miranda and M. Pizarro at the NTT.

MIDAS Memo

ESO Image Processing Group

1. MIDAS Environment Document

The first official version (1.0) of the MIDAS Environment document is now available. It contains complete documentation about the development of MIDAS application software for both FORTRAN and C. Besides a revision of the document, a chapter about Coding Standards for MIDAS applications and a table example programme have been added. This document will be the reference for anybody wanting to contribute software to MIDAS. Copies will be sent to all MIDAS sites automatically. Additional copies can be obtained from the Image Processing Group at ESO, contact Resy de Ruijscher.

2. MIDAS Directory Structure

A revision of the MIDAS directory structure has been made to provide a clear separation between the Core system and all other application software. A standard directory structure for contributed packages is defined to enable